VARIABLE ANGLE TOW COMPOSITES FOR LIGHTWEIGHT AND SUSTAINABLE ABRIDGE DESIGN

Francesco S. Liguori[1], Giovanni Zucco[2] and Antonio Madeo[1]

[1] DIMES, University of Calabria, Ponte P. Bucci Cubo 42b, 87036 Rende (Cosenza), Italy
[2] School of Engineering and Bernal Institute, University of Limerick, Limerick, Ireland

Keywords: FRP bridges, Variable Angle Tow, buckling, composite structures.

ABSTRACT

The increasing use of composite materials in civil structures has led to a demand for designs that reduce environmental impact, extend service life and save costs. This study proposes the use of Variable Angle Tow (VAT) composite laminates to further improve the structural efficiency of civil structures, particularly bridge girders. VAT composite laminates have the unique ability to change fibre orientation pointwise over the structure, providing enhanced stiffness tailoring capabilities compared to traditional laminates where fibre angles are constant.

To the best of our knowledge, this is the first study to investigate the use of VAT composite laminates in civil structures. Previous research has shown the success of VAT composites in aerospace engineering, where they have been used to tailor structures' stiffness and optimise their postbuckling behaviour. In this study, we show that the use of VAT composite laminates in bridge girders improves their buckling and postbuckling behaviours, increases their overall stiffness, and outperforms traditional straight fibre laminates.

Numerical investigations using both in-house and commercial finite element software were conducted to assess the benefits of VAT composite laminates. Results from a multi-objective optimisation for different spans show that VAT composite laminates provide superior performance compared to traditional straight fibre laminates, thereby opening up new design scenarios for bridge structures.

1 Introduction

The deteriorating conditions of bridges and their maintenance is a growing concern worldwide, and highway agencies have recognised those as the most complex problems in transportation infrastructure [1]. The maintenance of existing bridges and the increasing demand for new infrastructures, which have fast installation time and superior mechanical properties compared to those realised with traditional civil engineering materials, such as concrete and steel, led researchers to consider innovative solutions [2]. Composite materials represent a viable alternative [3], thanks to their high stiffness- and strength-to-weight ratios, excellent fatigue and corrosion resistance, faster installation time, and reduced maintenance costs [4]. Composites also offer superior resistance to environmental degradation compared to traditional building materials [5] and stand as a sustainable option for constructions [6].

In 1998, the New York State Department of Transportation replaced a deteriorated bridge on a high federal highway using a fibre-reinforced plastic (FRP) slab in significantly less time than a conventional bridge project [7]. Later, several studies showed the technical advantages and economic benefits of using composite materials in structural civil engineering applications. In particular, researchers initially investigated the viability of using composite materials together with traditional materials [8, 9]. In this regard, Ekenel et al. [10] enhanced the flexural fatigue behaviour of reinforced concrete beams by using FRP fabric and pre-cured laminate systems. Dagher et al. [11] used FRP tubular, concrete-filled arches to support bridges. An interesting application of FRP in bridges consists of realising their structural components entirely with these materials. Gutiérrez et al. [12], who realised a vacuum-infused FRP girder with a closed trapezoidal shape, gave a milestone work in this context. Later, Siwoski et al. [13] designed and manufactured a vacuum-infused, glass-carbon hybrid tub girder with a highly optimised cross-section for bridge applications. This work assessed the girder's performance through laboratory experiments, finite-element analysis (FEA) and field load testing. Finally, the findings presented in [13] led to the design and construction of a 22 m-long simple span bridge in Poland. Davids et al. [14] recently developed and implemented a lightweight, quickly erected, hybrid glass-carbon FRP girder for short- and medium-span bridges with composite concrete decks. In 2020, that girder was used for constructing a 22.9 m-long bridge project in Maine, USA. Field results showed the structural efficiency of the girder and its reduced transportation and erection requirements were shown.

The FRP structural components used in bridge engineering present in the literature are made of pultruded composites or straight-fibre laminates. However, more innovative technologies to manufacture composite materials have been proposed and investigated in the last decades. Among them, an interesting technology is represented by variable stiffness composite laminates, which enlarge the design space of straight-fibre laminates by changing the stiffness pointwise over the structure. One of the most successful way of realising variable stiffness composite laminates is the Variable Angle Tow (VAT) technology [15, 16, 17]. In VAT composite laminates, fibres draw curvilinear paths thereby enhancing stiffness tailoring capabilities with respect to straight-fibre laminates where fibre angles are constant.

VAT composites have been successfully used in aerospace engineering to tailor the structural stiffness and enhance their linear elastic response, reduce buckling phenomena, and optimise postbuckling behaviour [18, 19, 20]. For example, Daghighi et al. [21] used VAT composite laminates to suppress ineffective bending stresses in pressure vessels, which leads to efficient, lightweight design solutions. Exploiting VAT composite laminates, Liguori et al. [22] increased up to 29% the buckling load of a composite wingbox (i.e. the main structural component of an aircraft wing) of a commercial aircraft for medium-range flights [23].

To the best of the authors' knowledge, VAT composite laminates have never been used in civil engineering applications. Inspired by the successful examples achieved through this technology in aerospace engineering, this work proposes the exploitation of tow steering also in structural engineering. In particular, an initial design of a FRP bridge girder is presented that takes advantage from the superior performance of VAT composite laminates and introduces this new technology into civil engineering applications.

Starting from a commercial glass FRP girder [24], it is shown how the introduction of VAT composite laminates improves buckling and postbuckling behaviours and increases the overall stiffness. A parametric analysis is conducted to study the influence of different fibre paths on the linear static, buckling, and geometrically nonlinear elastic response for different bridge spans and loading conditions. A FE model constructed in Abaqus [25] is used to this end. Then, for the same geometries, an in-house FE software using a mixed element is coupled to a genetic algorithm to conduct a multi-objective optimisation of the layups. In particular, for a fixed span length and loading condition, the multi-objective optimisation soaks for the VAT layup that minimises the linear elastic static deflection and maximises its buckling load. Subsequently, the fully geometrically nonlinear response of the optimised girder is investigated. For all the girders under consideration, the optimal results are compared with those obtained by optimising unidirectional fibres. Comparison shows that optimised girders with VAT layups performed better than those optimised with unidirectional fibres in all cases.

The paper is organised as follows. A description of the FRP bridge and the proposed VAT girder is given in Section 2. The numerical model used for analysing the VAT structure is presented in Section 3. The parametric study conducted on the VAT girder is discussed in Section 4. Finally, conclusions are drawn in Section 5.

2 FRP girder bridge with VAT laminates

This Section describes a bridge made with conventional FRP composite material. Then, some insights into the VAT technology are given, and a VAT version of the FRP girder is proposed.

Table 1: Material properties of the glass FRP material adopted in the numerical simulations.

E_1 [GPa]	E_2 [GPa]	ν_{12}	G_{12} [GPa]	G_{23} [GPa]
30	10	0.3	5	3.5

2.1 FRP girder

A bridge composed of FRP girders, as shown in Fig. 1, is considered. In particular, the girder is the Double Web Beam (DWB) developed by Strongwell in Bristol in the late 1990s [24], which is a stand-alone pultruded girder that can be used in spans of up to 18 m and is made of a hybrid of glass and carbon fibres. The girder is available in two sizes. The smaller (named 8" DWB) was first used in 1997 in Tom's Creek Bridge, having a span of 5.5 m [26], while the larger one (named 36" DWB) in the 11.9 m long Route 601 bridge in 2001 [27]. This work considers the latter section, specifically designed for vehicular bridges, whose dimensions are given in Fig. 2. For simplicity and due to the scope of this work, instead of the actual hybrid material, it is assumed that the girder is made only of glass FRP whose properties are shown in Table 1.

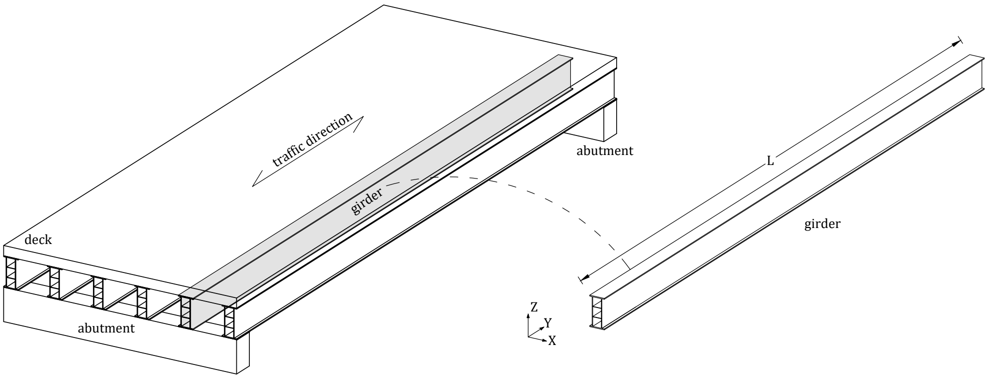

Figure 1: FRP bridge and a detail of a single girder [24].

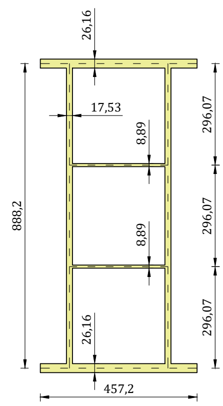

Figure 2: Cross section of the 36" DWB FRP [24] girder. All the lengths are expressed in mm.

2.2 VAT laminates

VAT composites are characterised by fibre orientations varying spatially over the structure. The fibre variation can be described with different expressions. A commonly-used choice is represented by the linear variation proposed by Gürdal and Olmedo in [28]. In such a case, considering a structure's plane,

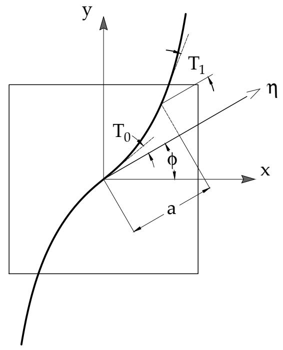

Figure 3: Fibre path parameterisation according to the linear variation proposed by Gürdal and Olmedo [28].

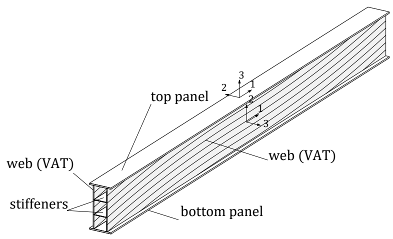

Figure 4: Schematic of the proposed FRP girder where VAT laminates are used in the web.

the fibre orientation linearly varies along one direction of that plane as

$$\vartheta[\eta] = \varphi + \left(\frac{T_1 - T_0}{a}\right)|\eta| + T_0 \tag{1}$$

where η is an abscissa measured along a direction rotated of φ according to Fig. 3, T_0 and T_1 are respectively the fibre orientations at the point where $\eta = 0$ and the point where $\eta = a$, measured with respect to φ. A layer using this fibre path parameterisation is indicated with the notation $\varphi\langle T_0, T_1\rangle$.

Nonlinear variations of the fibre orientation provide further possibilities for exploiting the VAT technology [19].

2.3 The VAT girder

Starting from the commercial FRP girder described in Section 2.1, a VAT version is herein proposed. The VAT girder has the same cross-section as shown in Fig. 2, and its web panels are made of VAT laminates (see Fig. 4).

With the aim of not modifying the inertia of the cross section with the respect to an horizontal axis, top and bottom skins and stiffeners are kept as SF composites with fibre orientations aligned with the beam axis ($0°$, measured with respect to the local reference system given in Fig. 4).

The linear fibre variation described by Eq. (1) is adopted. Figure 5 shows a girder side view in which it is displayed the fibre orientation of the VAT web. For each Vat web, the steering direction is the longitudinal axis of the girder, namely $\varphi = 0$, with respect to the web's local reference system. For $Y = 0$ and $Y = L$, the fibre orientation equals T_1, while at the plate centre its value is T_0. According to Eq. (1), the abscissa η coincides with the local reference axis e_1 and is measured starting from the plate centre, while $a = L/2$. Conversely, it is possible to observe that the fibre orientation does not change with Z. According to Gürdal and Olmedo notation, a web VAT lamina is indicated as $0\langle T_0, T_1\rangle$.

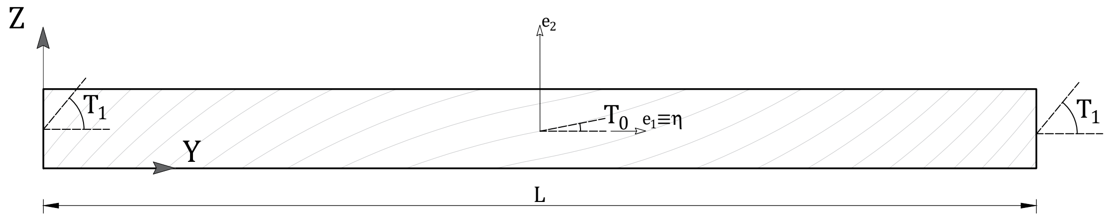

Figure 5: VAT fibre orientations of the girder web, linearly varying from T_1 at $Y = 0$ to T_0 at $Y = L/2$.

3 Numerical model

The structural performance of the proposed VAT girder is analysed numerically. The adopted model uses the commercial software Abaqus [25]. In this way, the analysis is conducted using a well-established numerical tool, and the presented results can be easily reproduced.

In Abaqus, shell FE are used to discretise the structure. In particular, S8R is adopted, which is an eight-nodes FE with drilling rotations based on the Mindlin-Reissner shell model and FSDT. To model the VAT laminates, a Python script is developed for assigning the fibre orientation at each element on the basis of the value at its centroid calculated with Eq. 1.

3.1 Boundary conditions and load cases

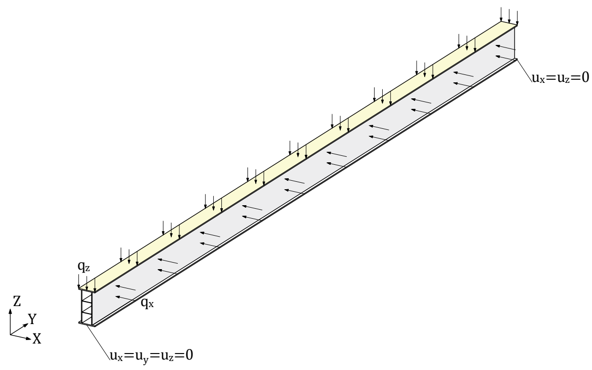

Figure 6: Boundary conditions and loads.

The girder is considered to be simply supported at the bottom edge of both its end sections, as shown in Fig. 6. Two different loading conditions are analysed. The first loading condition, indicated as load case A, considers only a vertical load q_z, uniformly distributed over the top panel. Whereas the second loading condition, indicated as load case B, considers only a horizontal load q_x, uniformly distributed over the left web.

4 Parametric analysis

In this Section, a parametric analysis is conducted to study the influence of different VAT configurations on the girder structural response. Three lengths for the girder, L, are considered, namely 10, 15 and 20 m. Two loading conditions are analysed separately. In particular, a surface load with $q_z = -10kN/m^2$ and $q_y = 0$ is used for case A, while, for Case B, $q_z = 0$ and $q_x = 10kN/m^2$.

For each length and loading condition, the laminate varies for the VAT girder. More precisely, an eight-layers layup $[\pm 0\langle 0|\vartheta\rangle]_{2S}$ is considered on both the girder's webs, with ϑ ranging from $0°$ to $90°$. To maximise the stiffness with respect to the horizontal axis, the fibre orientation at half of the beam length is fixed at $0°$.

To better understand the improvements given by the VAT technology to the structural response of the girder, the results obtained for the VAT configurations are compared with those of SF laminates where $[\pm\vartheta]_{2S}$. Additionally, a Quasi Isotropic (QI) laminate ($[\pm 45|90|0]_S$) is considered as the baseline.

In the parametric study, the following quantities are evaluated: the translations of point A (u_z^A and u_x^A), located in the centroid of the bottom panel, obtained from a linear elastic static analysis; the three lowest buckling loads (λ_1, λ_2 and λ_3) evaluated with a linear eigenvalue analysis; equilibrium paths evaluated using a path-following Riks analysis.

With the aim of presenting results obtained with a well-established commercial software, the results obtained with Abaqus are presented in this Section.

4.1 Load case A: vertical loads

For $L = 10m$, Table 2 shows the results of the parametric study where ϑ angle varies and compares the linear deflection and the buckling loads obtained for VAT and SF laminates. It is worth observing that for the VAT laminates, the linear deflection has small variations with respect to the fibre orientation, with a best value of 3.41 mm obtained when $\vartheta = 45°$. This aspect is explainable by the fact that the fibre orientations vary from $45°$ at the girder's extremities to $0°$ at its middle. Then, with respect to the case when fibres at $0°$, the shear contribution to deflection is reduced.

Conversely, for the SF laminates the deflection increases with increasing ϑ, and its best value that equals 3.52 mm is obtained for $\vartheta = 0°$. Therefore, by comparing the lowest deflection obtained for the VAT layups with the lowest deflection obtained for the SF layups, it is found that the VAT girder exabits a deflection 3.37% smaller than that of the SF girder.

Regarding the buckling loads, Table 2 shows that VAT significantly increases them, and the highest value is obtained when ϑ equals $90°$. Similarly, for the SF laminates, the buckling loads increase with increasing ϑ, and the best solution is still obtained for $\vartheta = 90°$. However, for the SF laminates, when the buckling performance improves, the deflection increases. Contrarily, with VAT laminates, it is possible to improve both the linear elastic and buckling behaviours simultaneously. This aspect is more evident from the graphs in Fig. 8a, which display the linear displacements and the first lowest buckling loads for both the VAT and SF layups normalised with respect to the QI case.

Therefore, when $L = 10$ m, the VAT laminates give clear advantages over the SF laminates, and this finding is explained by the presence of fibres at $0°$ in the middle part of the girder which reduces its linear elastic static deflection. Conversely, orientations between $45°$ and $90°$ are required near the girder's ends to increase the buckling loads and reduce the contribution to the static deflection given by the shear load. Then, thanks to the possibility given by VAT technology of varying the fibre orientation in the same layer, it is possible to satisfy both those requirements to enhance the linear elastic static and buckling behaviours simultaneously, while the same is not possible with SF laminates.

A similar behaviour is observed for bigger values of L. Tables 3 and 4 show the deflection and the three lowest buckling loads for $L = 15$ m and $L = 20$ m, respectively. For $L = 15$ m and $L = 20$ m, the linear static deflections and the first buckling load at different values of ϑ, normalised on the corresponding values obtained for the QI girders, are shown in Figs. 8b and 8c, respectively. Therefore, with the VAT technology, also in these cases, it is possible to increase the buckling safety factor while keeping low the linear deflection.

It is well known [29, 30] that the linear buckling loads are not generally proper indicators of structural safety against geometrically nonlinear phenomena. For this reason, fully geometrically nonlinear elastic static analyses are conducted to assess the structural behaviour of the VAT girders. To conduct these analyses, for each girder under consideration, a small imperfection with shape as its first buckling mode is introduced to trace the bifurcated branch.

For all the values of L under consideration, each graph in Fig. 7 shows the equilibrium paths as a function of u_Z^A for different values of ϑ. The equilibrium path of each girder is characterised by a slightly unstable initial post-critical behaviour after the limit load. VAT layups do not modify the shape of the equilibrium paths with respect to those obtained for the QI girders. Still, they significantly increase

Table 2: Results of the parametric analysis for the girder with $L = 10$ m subjected to load case A.

	VAT ($[0 \pm \langle 0\|\vartheta\rangle]_{2S}$)				SF ($[\pm\vartheta]_{2S}$)			
ϑ	u_z^A	λ_1	λ_2	λ_3	u_z^A	λ_1	λ_2	λ_3
90	-3.55	16.04	40.28	43.27	-4.11	15.80	39.37	43.12
75	-3.47	15.43	40.01	42.89	-4.05	15.46	39.78	42.83
60	-3.42	14.16	37.95	40.66	-3.94	14.33	38.71	40.87
45	-3.41	12.68	33.81	35.98	-3.82	12.79	34.78	36.32
30	-3.44	11.54	29.08	30.48	-3.65	11.56	29.69	30.74
15	-3.49	10.91	25.51	26.39	-3.53	10.91	25.70	26.48
0	-3.52	10.71	24.15	24.86	-3.52	10.71	24.15	24.86
QI	-3.74	13.33	34.28	36.13	-3.74	13.33	34.28	36.13

Table 3: Results of the parametric analysis for the girder with $L = 15$ m subjected to load case A.

	VAT ($[0 \pm \langle 0\|\vartheta\rangle]_{2S}$)				SF ($[\pm\vartheta]_{2S}$)			
ϑ	u_z^A	λ_1	λ_2	λ_3	u_z^A	λ_1	λ_2	λ_3
90	-16.68	9.13	25.22	27.75	-19.27	8.56	23.58	27.42
75	-16.36	8.96	24.97	27.73	-19.10	8.46	24.30	27.53
60	-16.09	8.41	23.79	26.52	-18.73	8.03	24.50	26.60
45	-15.89	7.67	21.57	23.73	-18.09	7.39	22.54	23.88
30	-15.79	7.05	18.85	20.33	-17.03	6.91	19.42	20.44
15	-15.80	6.69	16.67	17.65	-16.11	6.66	16.84	17.69
0	-15.84	6.57	15.80	16.62	-15.84	6.57	15.80	16.62
QI	-17.56	7.74	22.00	23.74	-17.56	7.74	22.00	23.74

Table 4: Results of the parametric analysis for the girder with $L = 20$ m subjected to load case A.

	VAT ($[0 \pm \langle 0\|\vartheta\rangle]_{2S}$)				SF ($[\pm\vartheta]_{2S}$)			
ϑ	u_z^A	λ_1	λ_2	λ_3	u_z^A	λ_1	λ_2	λ_3
90	-51.49	5.41	14.96	18.95	-59.35	4.89	13.73	15.49
75	-50.57	5.39	14.85	18.99	-58.99	4.88	14.26	15.52
60	-49.68	5.16	14.51	18.78	-58.05	4.73	14.95	15.69
45	-48.92	4.79	13.88	17.11	-56.02	4.47	14.88	16.22
30	-48.40	4.47	12.95	14.87	-52.50	4.30	13.73	14.99
15	-48.18	4.27	11.89	13.05	-49.27	4.23	12.13	13.09
0	-48.17	4.20	11.39	12.35	-48.17	4.20	11.39	12.35
QI	-54.16	4.68	14.44	16.86	-54.16	4.68	14.44	16.86

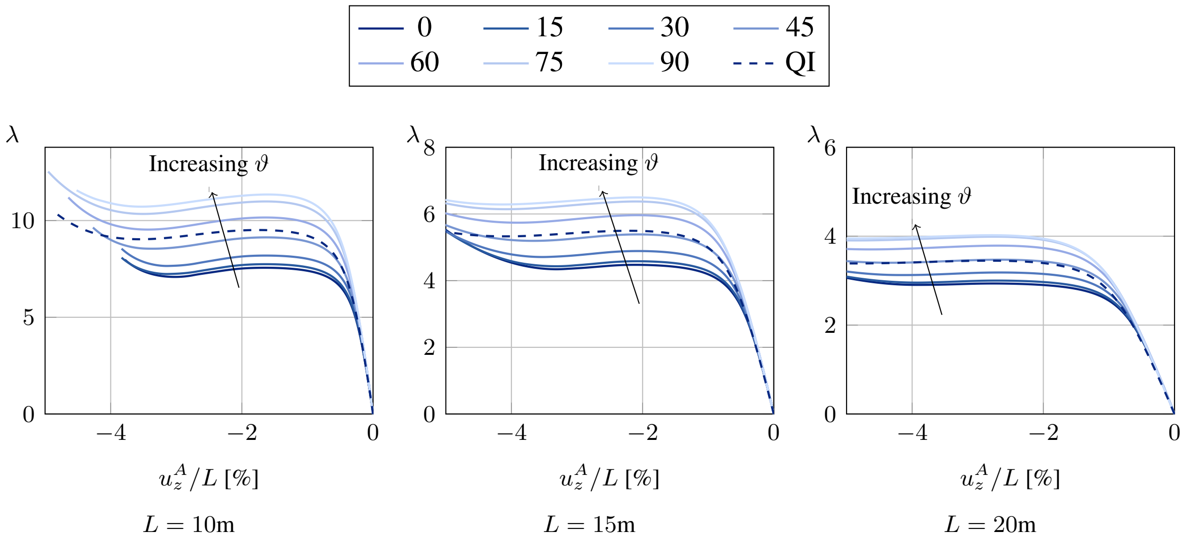

Figure 7: For the VAT girder with layup $[0 \pm \langle 0|\vartheta\rangle]_{2S}$, equilibrium paths for different values of ϑ.

the limit load and, therefore, the girders' loading bearing capability. The best solution is obtained for $\vartheta = 90°$. Finally, it is worth noting that VAT layups increase the torsional stiffness, improving the buckling resistance without modifying the pre-critical behaviour.

4.2 Load case B: horizontal loads

When subjected to load case B, the girder undergoes a uniform horizontal load, simulating wind actions on the bridge. Table 5 shows the results obtained when $L = 10$ m. Using VAT leads to a contemporary reduction of the horizontal translation and an increase in the buckling loads. This result cannot be achieved with SF laminates, for which the buckling behaviour improves at the cost of a displacement increase. In particular, the best VAT solution is obtained for $\vartheta = 90°$ and gives a reduction of the 12% of the displacement and an increase of the first buckling load of 80%, if compared with a $[0]_S$ SF layup. The advantages of using VAT instead of SF laminates are also observed in Fig. 8d, showing how the linear solution and the first buckling change with ϑ for both the VAT and SF configurations.

For $L = 15$ m, Table 6 and Fig. 8b show that the VAT technology is still capable of increasing the buckling load of about 80% with respect to a $[0]_S$ SF layup, even though in this case the linear displacement is almost constant with ϑ. Then, SF laminates can improve the buckling resistance, but at the price of an increase of the displacement up to 35%. Since, for such structures, displacement limits drive their design, a significant decay of linear elastic performance is not acceptable.

The same considerations as for the girders with $L = 10$ m and $L = 15$ m hold for those with $L = 20$ m whose results are shown in Table 7 and Fig. 8c. For the VAT girders, the first buckling load increases up to 55% for ϑ ranging from 0° to 90°, but the linear displacement increases by about 10%. However, the linear displacement increase obtained with SF laminates is about 35%. Therefore, the VAT technology still provides better results than SF laminates.

5 Conclusions

In this work, a technology successfully employed in aeronautical engineering has been proposed in a civil engineering context for the first time. It consists in composites laminates, called Variable Angle Tow (VAT), in which fibres draw curvilinear paths whose orientations change pointwise over the structure. Consequently, designers can use more variables to tailor the stiffness to the desired structural response, thereby leading to optimised structures. We have proposed the use of VAT laminates in FRP bridges. In fact, the use of composite materials in bridges is a promising and still open field and is giving the possibility of designing lightweight structures with low maintenance costs and high mechanical

Table 5: Results of the parametric analysis for the girder with $L = 10$ m subjected to load case B.

	VAT ($[0 \pm \langle 0 \vert \vartheta \rangle]_{2S}$)				SF ($[\pm\vartheta]_{2S}$)			
ϑ	u_z^A	λ_1	λ_2	λ_3	u_x^A	λ_1	λ_2	λ_3
90	-74.95	7.57	7.71	12.42	-90.07	7.54	7.67	12.37
75	-74.89	7.50	7.68	12.03	-90.58	7.48	7.64	11.99
60	-76.56	7.04	7.23	11.09	-91.81	7.07	7.26	11.12
45	-79.60	6.13	6.29	9.65	-91.93	6.20	6.36	9.74
30	-82.64	5.13	5.23	8.19	-89.32	5.19	5.30	8.26
15	-84.52	4.44	4.51	7.19	-86.23	4.46	4.53	7.22
0	-85.13	4.19	4.25	6.85	-85.13	4.19	4.25	6.85
QI	-85.99	6.14	6.27	9.78	-85.99	6.14	6.27	9.78

Table 6: Results of the parametric analysis for the girder with $L = 15$ m subjected to load case B.

	VAT ($[0 \pm \langle 0 \vert \vartheta \rangle]_{2S}$)				SF ($[\pm\vartheta]_{2S}$)			
ϑ	u_z^A	λ_1	λ_2	λ_3	u_x^A	λ_1	λ_2	λ_3
90	-263.48	5.02	5.11	6.51	-343.02	5.01	5.09	8.22
75	-257.44	4.98	5.09	6.47	-342.49	4.97	5.07	7.97
60	-253.79	4.68	4.80	6.43	-338.09	4.70	4.82	7.39
45	-252.74	4.09	4.19	6.39	-321.03	4.12	4.22	6.47
30	-253.03	3.42	3.48	5.45	-289.59	3.45	3.51	5.48
15	-253.30	2.95	2.99	4.78	-262.56	2.96	3.00	4.79
0	-253.41	2.78	2.82	4.55	-253.41	2.78	2.82	4.55
QI	-296.27	4.08	4.16	6.49	-296.27	4.08	4.16	6.49

Table 7: Results of the parametric analysis for the girder with $L = 20$ m subjected to load case B.

	VAT ($[0 \pm \langle 0 \vert \vartheta \rangle]_{2S}$)				SF ($[\pm\vartheta]_{2S}$)			
ϑ	u_z^A	λ_1	λ_2	λ_3	u_x^A	λ_1	λ_2	λ_3
90	-744.98	3.62	3.62	3.75	-997.44	3.75	3.81	5.65
75	-722.03	3.61	3.61	3.72	-993.55	3.72	3.79	5.84
60	-701.57	3.50	3.59	3.59	-971.83	3.51	3.60	5.53
45	-685.55	3.06	3.14	3.58	-904.95	3.08	3.16	4.84
30	-674.42	2.56	2.61	3.56	-791.95	2.58	2.63	4.10
15	-667.77	2.21	2.24	3.56	-697.59	2.22	2.25	3.58
0	-665.61	2.08	2.11	3.40	-665.61	2.08	2.11	3.40
QI	-830.45	3.05	3.12	4.86	-830.45	3.05	3.12	4.86

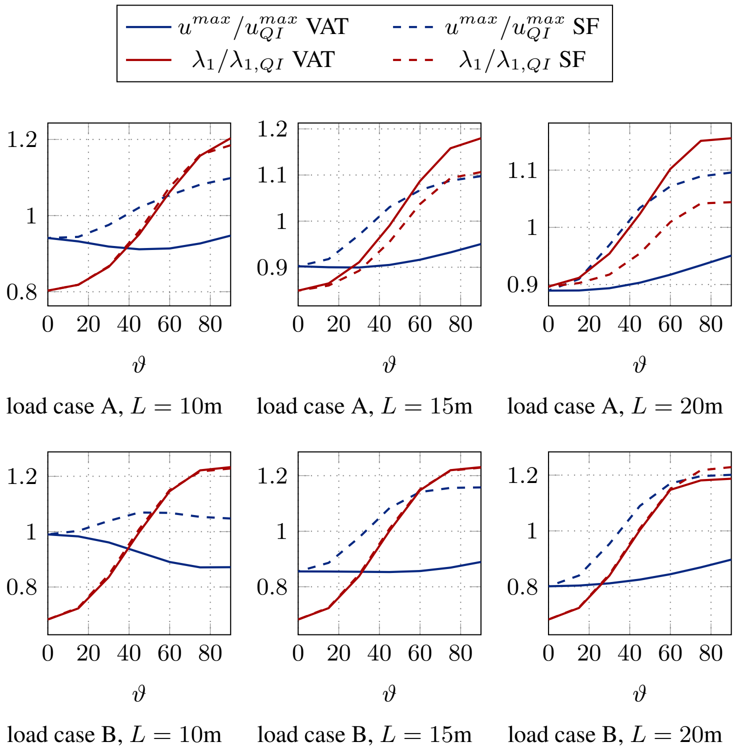

Figure 8: For the vertical and horizontal loading conditions, variation of the normalised maximum linear deflection and first buckling load for different values of ϑ.

performance. To test the effectiveness of using VAT laminates, a commercial FRP bridge girder has been modified by introducing VAT panels in its webs. A parametric study has been carried out to analyse the variation of the linear and geometrically nonlinear structural response with the fibre orientations. Results have highlighted the superior performance provided by VAT if compared to more traditional laminates with straight fibres. In particular, VAT laminates allow to increase the buckling resistance up to 80% with equal or better deflections and without adding extra material.

REFERENCES

[1] Abdul-Hamid Zureick, B. Shih, and E. Munley. Fiber-reinforced polymeric bridge decks. *Structural Engineering Review*, 7:257–266, 1995.

[2] M. (Ed.) Zoghi. *The International Handbook of FRP Composites in Civil Engineering (1st ed.)*. CRC Press, 2013.

[3] Thomas Keller. Recent all-composite and hybrid fibre-reinforced polymer bridges and buildings. *Progress in Structural Engineering and Materials*, 3(2):132–140, 2001.

[4] Hafiz Tauqeer Ali, Roya Akrami, Sakineh Fotouhi, Mahdi Bodaghi, Milad Saeedifar, Mohammad Yusuf, and Mohamad Fotouhi. Fiber reinforced polymer composites in bridge industry. *Structures*, 30:774–785, 2021.

[5] Prakash Kumar, K Chandrashekhara, and Antonio Nanni. Structural performance of a frp bridge deck. *Construction and Building Materials*, 18(1):35–47, 2004.

[6] Yeou-Fong Li, Habib Armel Meda, and Walter Chen. The design and analysis of internally stiffened gfrp tubular decks—a sustainable solution. *Sustainability*, 10(12), 2018.

[7] Sreenivas Alampalli, Jerome O'Connor, and Arthur P Yannotti. Fiber reinforced polymer composites for the superstructure of a short-span rural bridge. *Composite Structures*, 58(1):21–27, 2002.

[8] Xingxing Zou, Hongwei Lin, Peng Feng, Yi Bao, and Jingquan Wang. A review on frp-concrete hybrid sections for bridge applications. *Composite Structures*, 262:113336, 2021.

[9] Arvid Hejll, Björn Täljsten, and Masoud Motavalli. Large scale hybrid frp composite girders for use in bridge structures—theory, test and field application. *Composites Part B: Engineering*, 36(8):573–585, 2005.

[10] Mahmut Ekenel, Andrea Rizzo, John J. Myers, and Antonio Nanni. Flexural fatigue behavior of reinforced concrete beams strengthened with frp fabric and precured laminate systems. *Journal of Composites for Construction*, 10(5):433–442, 2006.

[11] Habib J. Dagher, Daniel J. Bannon, William G. Davids, Roberto A. Lopez-Anido, Edwin Nagy, and Keenan Goslin. Bending behavior of concrete-filled tubular frp arches for bridge structures. *Construction and Building Materials*, 37:432–439, 2012. Non Destructive Techniques for Assessment of Concrete.

[12] E. Gutiérrez, S. Primi, J. M. Mieres, and I. Calvo. Structural testing of a vehicular carbon fiber bridge: Quasi-static and short-term behavior. *Journal of Bridge Engineering*, 13(3):271–281, 2008.

[13] Tomasz Siwowski, Maciej Kulpa, Mateusz Rajchel, and Pawel Poneta. Design, manufacturing and structural testing of all-composite frp bridge girder. *Composite Structures*, 206:814–827, 2018.

[14] William G. Davids, Anthony Diba, Habib J. Dagher, Dante Guzzi, and Andrew P. Schanck. Development, assessment and implementation of a novel frp composite girder bridge. *Construction and Building Materials*, 340:127818, 2022.

[15] C.S. Lopes, P.P. Camanho, Z. Gürdal, and B.F. Tatting. Progressive failure analysis of tow-placed, variable-stiffness composite panels. *International Journal of Solids and Structures*, 44(25):8493–8516, 2007.

[16] C.S. Lopes, Z. Gürdal, and P.P. Camanho. Variable-stiffness composite panels: Buckling and first-ply failure improvements over straight-fibre laminates. *Computers & Structures*, 86(9):897–907, 2008. Composites.

[17] D.M. Li, Carol A. Featherston, and Zhangming Wu. An element-free study of variable stiffness composite plates with cutouts for enhanced buckling and post-buckling performance. *Computer Methods in Applied Mechanics and Engineering*, 371:113314, 2020.

[18] Giovanni Zucco and Paul M. Weaver. Post-buckling behaviour in variable stiffness cylindrical panels under compression loading with modal interaction effects. *International Journal of Solids and Structures*, 203:92–109, 2020.

[19] Francesco S. Liguori, Giovanni Zucco, Antonio Madeo, Giovanni Garcea, Leonardo Leonetti, and Paul M. Weaver. An isogeometric framework for the optimal design of variable stiffness shells undergoing large deformations. *International Journal of Solids and Structures*, 2020.

[20] Giovanni Zucco, Mohammad Rouhi, Vincenzo Oliveri, Enzo Cosentino, Ronan M. O'Higgins, and Paul M. Weaver. Continuous tow steering around an elliptical cutout in a composite panel. *AIAA Journal*, 59(12):5117–5129, 2021.

[21] Shahrzad Daghighi, Giovanni Zucco, Mohammad Rouhi, and Paul M. Weaver. Bend-free design of super ellipsoids of revolution composite pressure vessels. *Composite Structures*, 245:112283, 2020.

[22] Francesco S. Liguori, Giovanni Zucco, Antonio Madeo, Domenico Magisano, Leonardo Leonetti, Giovanni Garcea, and Paul M. Weaver. Postbuckling optimisation of a variable angle tow composite wingbox using a multi-modal Koiter approach. *Thin-Walled Structures*, 138:183 – 198, 2019.

[23] Vincenzo Oliveri, Giovanni Zucco, Daniël Peeters, Gearóid Clancy, Robert Telford, Mohammad Rouhi, Ciarán McHale, Ronan M. O'Higgins, Trevor M. Young, and Paul M. Weaver. Design, manufacture and test of an in-situ consolidated thermoplastic variable-stiffness wingbox. *AIAA Journal*, 57(4):1671–1683, 2019.

[24] Strongwell. Extren DWG Design Guide. *Strongwell Corporation*, 2003.

[25] K. Hibbit and P. Sorenson. Abaqus analysis user's manual version 6.7. 2007.

[26] M. D. Hayes, J. J. Lesko, J. Haramis, T. E. Cousins, J. Gomez, and P. Masarelli. Laboratory and field testing of composite bridge superstructure. *Journal of Composites for Construction*, 4(3):120–128, 2000.

[27] Edgar Restrepo, Tommy Cousins, and Jack Lesko. Determination of bridge design parameters through field evaluation of the route 601 bridge utilizing fiber-reinforced polymer girders. *Journal of Performance of Constructed Facilities*, 19(1):17–27, 2005.

[28] Zafer Gurdal and Reynaldo Olmedo. In-plane response of laminates with spatially varying fiber orientations - variable stiffness concept. *AIAA Journal*, 31(4):751–758, 1993.

[29] Leonardo Leonetti, Francesco Liguori, Domenico Magisano, and Giovanni Garcea. An efficient isogeometric solid-shell formulation for geometrically nonlinear analysis of elastic shells. *Computer Methods in Applied Mechanics and Engineering*, 331:159 – 183, 2018.

[30] E.J. Barbero, A. Madeo, G. Zagari, R. Zinno, and G. Zucco. Imperfection sensitivity analysis of laminated folded plates. *Thin-Walled Structures*, 90:128 – 139, 2015.